ECCOMAS Congress 2016
VII European Congress on Computational Methods in Applied Sciences and Engineering
M. Papadrakakis, V. Papadopoulos, G. Stefanou, V. Plevris (eds.)
Crete Island, Greece, 5–10 June 2016

A MACRO-ELEMENT FORMULATION FOR ROCKING FLEXIBLE BODIES WITH A DEFORMABLE BASE

Evangelos Avgenakis and Ioannis N. Psycharis

School of Civil Engineering
National Technical University of Athens, Greece
Polytechnic Campus, Heroon Polytechniou 9, 15780 Zografou
e-mail: vavgen@outlook.com, ipsych@central.ntua.gr

Keywords: Rocking, Macro-element, Non-linear analysis

Abstract. *In recent years, an increased interest in the use of rocking members for the design of earthquake resistant structures is observed. As described in the literature, the use of rocking members leads to more resilient structural systems, since, in contrast to conventional members which develop damage and residual deformations, rocking members have the ability to re-center without significant damage, leading to increased structural safety and lower repair costs after a seismic event, while their yield-like response restrains the seismic forces acting on the structure.*

Although much research has been conducted on the response of rocking members, mainly regarding analytical solutions for free-standing rocking bodies with rigid bases and simplified guidelines for the design of structural rocking members, it is believed that there is a need for simple computational models, which can describe the response of rocking flexible members in structural systems more realistically.

In this paper, a new approach that is able to take into account the deformation along the height of the body and along the contact areas, especially required for cases of constrained structural members, is applied for the development of a generalized macro-element, which can be used in the context of a finite element program. The theoretical formulation of the problem is based on the solution of the normalized semi-infinite strip problem with random loads on its free side. The new macro-element is demonstrated using typical example problems and the results are compared with corresponding results obtained with Abaqus, showing excellent agreement. Concerning the required runtimes, the macro-element runs significantly faster compared to conventional finite element codes.

1 INTRODUCTION

The complex mechanics of the rocking motion of rocking bodies and structural members have attracted attention from the scientific community in recent years, although the phenomenon is known from ancient times, as many ancient monuments were built with members allowed to rock.

The rocking motion occurs when a member is unrestrained or at least partially restrained at its base, so that tensile stresses cannot be transmitted, as considered in classical structural mechanics. Given that the imposed forces are large enough, the rocking body detaches from the ground and rotates about one of its corners. The vertical force acts as the restoring force that tends to bring the body back to its original equilibrium position.

The inclusion of rocking members in real structures is considered a promising solution to the design of resilient structures. Conventional structural elements are designed to gradually yield and develop damage and residual deformations during an earthquake. Such an approach means that, after a seismic event, costly and time-consuming repairs of the building may be necessary. In contrast, the motion of rocking members is a yield-like response, able to limit the forces transmitted to the structure during an earthquake, without however developing significant damage, while the residual deformations are virtually non-existent. As as result, fewer repairs are needed after a seismic event in comparison to the conventional design.

Up to date, rocking members have been applied in case of bridge piers (e.g. the Rangitikei Railway Bridge [1]), while extensive analytical and experimental work has been performed on rocking shear walls in precast structures (e.g. [2], [3], [4]). Guidelines addressing this alternative seismic design have been published by several organizations ([5], [6], [7]), while in Eurocode 8 (EN 1998-1) [8], rocking is anticipated for large lightly reinforced walls during strong earthquakes.

Although various analytic solutions exist regarding the motion of the rigid rocking block (e.g. [9], [10], [11], [12]), as well as approximate formulas for the design of controlled rocking systems, few models exist for modeling the response of deformable rocking bodies (e.g. [13], [14], [15], [16]). These studies, however, consider only the deformability of the rocking member along its height, while the lower face, along which the contact with the base takes place, is considered rigid. As a result, rocking occurs around the corners of the bottom side. The main attempts that have been presented including the flexibility of the base concern the rocking of rigid bodies on a flexible foundation (e.g. [17], [18], [19], [20], [21], [22], among others). Computational approaches taking into account the deformability of the base of rocking members include [23], [24], [25], [26], [27].

In this paper, a new macro-element formulation is proposed, able to take into account both the deformability of the rocking member along its height and along the contact area with the base mat. The main idea behind the proposed approach is to assume a stress distribution acting on the section of the rocking interface, depending on the resultant forces on this interface, and try to predict the displacements of the rocking element due to this partial loading. To this end, the similarity between the original problem of the flexible rocking body and that of a cantilever, partially loaded on its free side with normal and shear stresses that model the ones acting on the contact region of the body while rocking (Fig. 1) is used. More information on the applied technique can be found in [28].

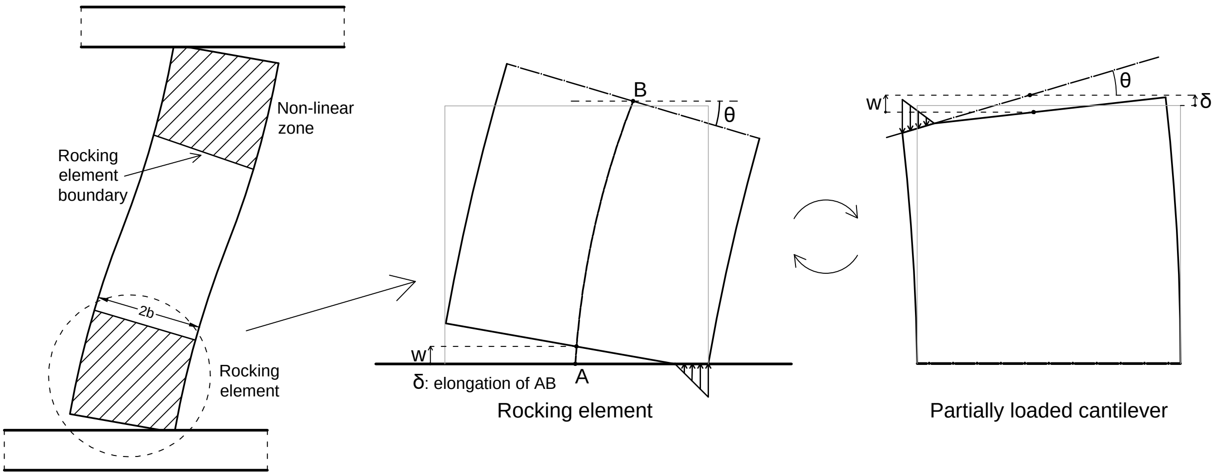

Figure 1: Rocking body and partially loaded cantilever analogy

2 NORMALIZED SEMI-INFINITE STRIP PROBLEM

In order to calculate the displacements of a cantilever due to partial loading on its free side, the spatial stress distribution near the loaded region has to be derived. From this stress distribution, an elongation profile across the member section can be found, from which the relative deformations of the element can be calculated.

The normal and shear stress distributions applied on the free side are separated into: *(i)* stresses produced by the resultant forces (axial force, shear force and moment); and *(ii)* self-equilibrating stresses. For the latter, since the effect of the self-equilibrating stresses is expected to vanish along the cantilever (rightmost diagram in Fig. 1), as the Saint-Venant assumption suggests, the easier semi-infinite strip problem is used instead. The stress distributions of the resultant forces are calculated according to the technical theory, so the use of a cantilever model is not necessary.

The general self-equilibrating stress problem for a semi-infinite strip of width $B = 2b$ is solved by first examining the normalized problem, which refers to a semi-infinite strip of $b = 1$ (Fig. 2).

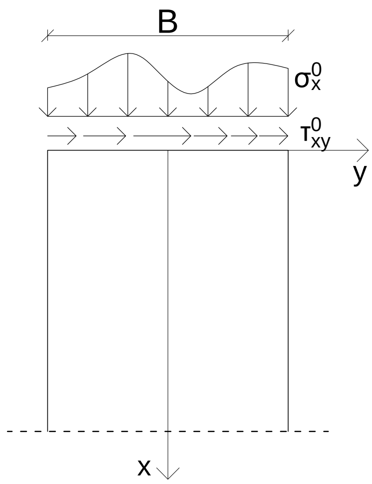

Figure 2: Semi-infinite strip normalized problem

The self-equilibrating stress distribution problem of the normalized semi-infinite strip is calculated with the method developed in [29], using stress functions of certain form. The problem considered is that of a semi-infinite strip $x \geq 0$, $-1 \leq y \leq 1$ with generalized stress distributions on the free side, $x = 0$ (Fig. 2).

In the proposed macro-element, the results produced for specific load distributions of interest are approximated by polynomial expressions, which are easier and faster to implement.

The free surface of the semi-infinite strip is assumed to be loaded in the interval $[-1, p-1]$, representing a contact region of length p of the corresponding rocking body (Fig. 3). The self-equilibrating stress distributions assumed for the free surface of the semi-infinite strip originate from the following stress distributions, similar to the contact stresses at the interface between the rocking body and the base, after the removal of resultant forces:

Normal stresses which have a triangular distribution. The maximum value is s at the edge, $y = -1$, while it becomes zero after length p, that is at $y = p - 1$.

Shear stresses which are assumed to have a parabolic distribution. Its values are zero at $y = -1$ and $y = p - 1$, while its maximum value t occurs at $y = 0.5p - 1$

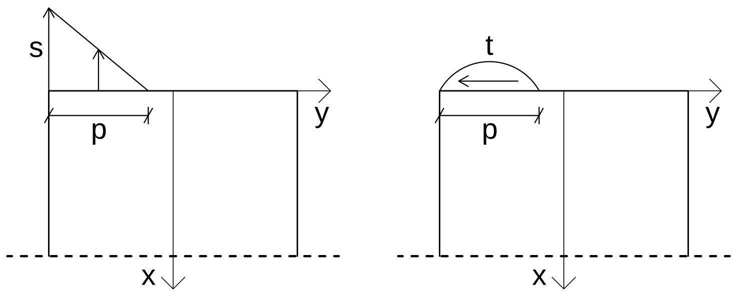

Figure 3: Semi-infinite strip normal (s) and shear (t) load distributions, for loaded region of length p

For the real problem, the interface between the body and the base mat remains flat. However, for the corresponding cantilever problem, the loaded region of the strip, although it remains close to flat, is not exactly flat. This causes problems when the elongation and the corresponding slope of a specific point on the loaded edge are used for the prediction of the axial elongation and the rotation of the body. For this reason, the elongation profile $u(y)$ of the fibers across the loaded region $[-1, -1+p]$ is interpolated by a linear function $g(y) = \delta + \theta y$ (Fig. 1), in which δ and θ are the predicted axial elongation and the top rotation of the normalized problem, respectively, taking into account the gap existing between the loaded and non-loaded surfaces (Fig. 1).

It can be shown that for the stress distributions examined, the displacement vector $\boldsymbol{U} = [\delta, \theta]^T$ can be very well approximated by the following expressions:

$$\boldsymbol{U} = \begin{Bmatrix} \dfrac{1}{E} \left(s\boldsymbol{V}_s^T + t\boldsymbol{V}_t^T \right) \boldsymbol{P}_6 \\ \dfrac{1}{E} \left(s\boldsymbol{R}_s^T + t\boldsymbol{R}_t^T \right) \boldsymbol{P}_6 \end{Bmatrix} \tag{1}$$

where

$$\boldsymbol{P}_6 = [p^6 \quad p^5 \quad p^4 \quad p^3 \quad p^2 \quad p \quad 1]^T \tag{2}$$

$$\boldsymbol{V}_t = \boldsymbol{V}_{t0} + \nu \boldsymbol{V}_{td} \tag{3}$$

$$\boldsymbol{R}_t = \boldsymbol{R}_{t0} + \nu \boldsymbol{R}_{td} \tag{4}$$

Table 1: Polynomial approximation constant term vectors

$\boldsymbol{V}_s$	$\boldsymbol{V}_{t0}$	$\boldsymbol{V}_{td}$	$\boldsymbol{R}_s$	$\boldsymbol{R}_{t0}$	$\boldsymbol{R}_{td}$
-0.1403784	0.14011296	-0.2542931	0.00789778	0.09467081	-0.1525667
1.07433528	-1.0383282	1.50541409	-0.0232445	-0.5696705	0.90318304
-3.2789455	3.14664208	-3.3275039	0.01957306	1.40705090	-2.0163212
5.21236206	-5.1023030	3.28205442	-0.0568735	-1.7749925	1.95898891
-5.0376812	5.24787880	-1.2327789	-0.2965314	1.46712898	-0.5395043
3.53446524	-4.2918559	0.41774356	1.58546025	-2.1973954	0.21059712
-1.5484860	2.32362124	-0.8192345	-1.6046083	2.38392244	-0.8115360

E and ν being Young's modulus and the Poisson ratio, respectively, and the polynomial constant term $\boldsymbol{V}_s$ and $\boldsymbol{R}_s$ (for the normal stress contribution) and $\boldsymbol{V}_{t0}, \boldsymbol{V}_{td}, \boldsymbol{R}_{t0}, \boldsymbol{R}_{td}$ (for the shear stress contribution) vectors given in Table 1.

Also, the flexibility matrix of the normalized problem $\boldsymbol{F_t} = \partial \boldsymbol{U} / \partial \boldsymbol{R}$, with $\boldsymbol{R} = [p, s, t]^T$, is calculated by the following expression:

$$\boldsymbol{F_t} = \frac{\partial \boldsymbol{U}}{\partial \boldsymbol{R}} = \begin{bmatrix} \frac{1}{E}\left(s\boldsymbol{V}_s^T + t\boldsymbol{V}_t^T\right) \boldsymbol{dP}_6 & \frac{1}{E}\boldsymbol{V}_s^T \boldsymbol{P}_6 & \frac{1}{E}\boldsymbol{V}_t^T \boldsymbol{P}_6 \\ \frac{1}{E}\left(s\boldsymbol{R}_s^T + t\boldsymbol{R}_t^T\right) \boldsymbol{dP}_6 & \frac{1}{E}\boldsymbol{R}_s^T \boldsymbol{P}_6 & \frac{1}{E}\boldsymbol{R}_t^T \boldsymbol{P}_6 \end{bmatrix} \tag{5}$$

where

$$\boldsymbol{dP}_6 = [6p^5 \quad 5p^4 \quad 4p^3 \quad 3p^2 \quad 2p \quad 1 \quad 0]^T \tag{6}$$

The predicted displacements derived from the semi-infinite strip problem were compared against results obtained with Abaqus. Two cases for various cantilever heights were considered, with constant width $B = 2$: in the first one, the rocking member was loaded on its top with a concentrated moment, while in the second one it was loaded with a concentrated horizontal force. Figures (4) and (5) present the comparison results in relation to the different contact lengths, p, which show that, generally, there is very good agreement between the results of the two methods, especially for more slender members.

3 A MACRO-ELEMENT FORMULATION

By combining the self equilibrating stresses and the resultant force contributions (Fig. 6), a macro-element algorithm is developed which accounts for the total response of the rocking member.

For the rocking macro-element formulation, the concept of the simply supported beam natural system will be used, which is based on the geometrically non-linear force-based beam-column element formulation proposed by Neuenhofer and Filippou [30]. This coordinate system without rigid body modes demands only relative displacement values and not absolute ones, thus enabling the use of relative displacements presented previously for the self-equilibrating stresses contribution. The equations for the transformation of the displacements and forces to and from the simply supported beam natural coordinate system can be found in [30].

For the normalized semi-infinite strip problem discussed in section 2, given the load parameter vector $\boldsymbol{R} = [p, s, t]^T$, the displacements $\boldsymbol{U}$ and the flexibility matrix $\frac{\partial \boldsymbol{U}}{\partial \boldsymbol{R}}$ can be evaluated, which refer to the cantilever-like reference system of the semi-infinite strip. However, in order to combine these results with the resultant force ones, these quantities have to be converted from and to a reference system of a simply supported beam.

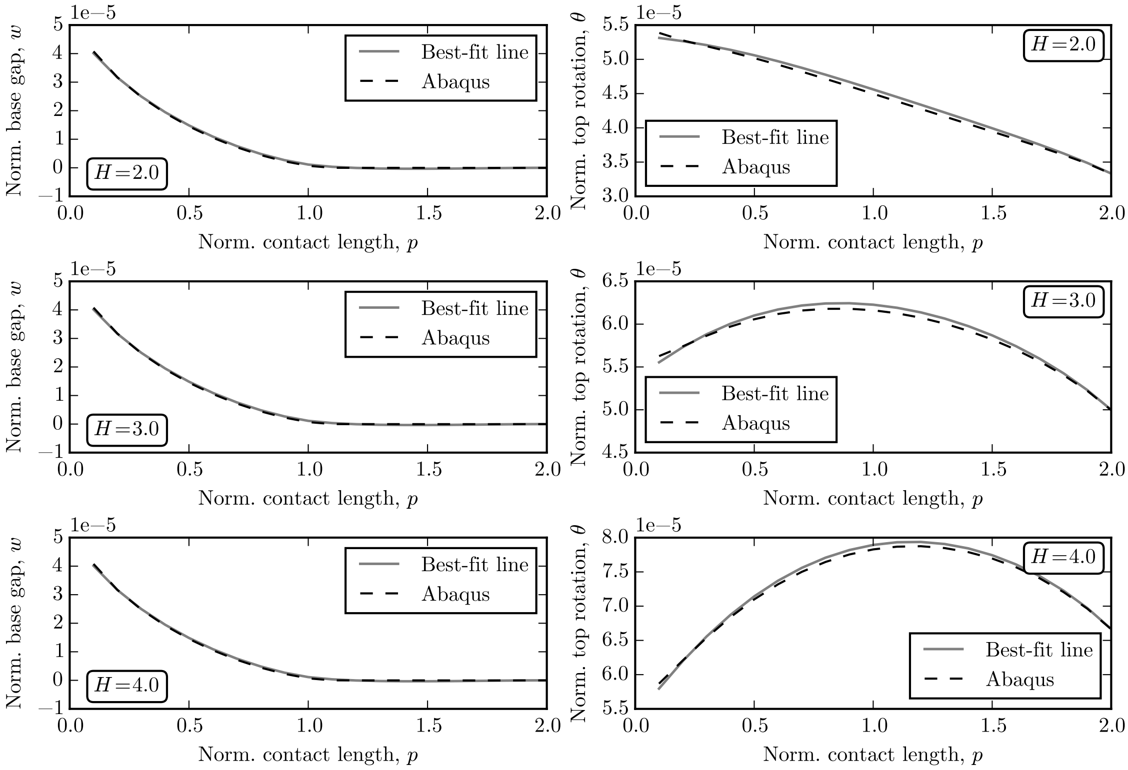

Figure 4: Rocking members with different heights loaded with a concentrated moment on their top: Central gap and top rotation versus the contact length at the bottom, p, and for $s = -1000, E = 30000000, \nu = 0.2$

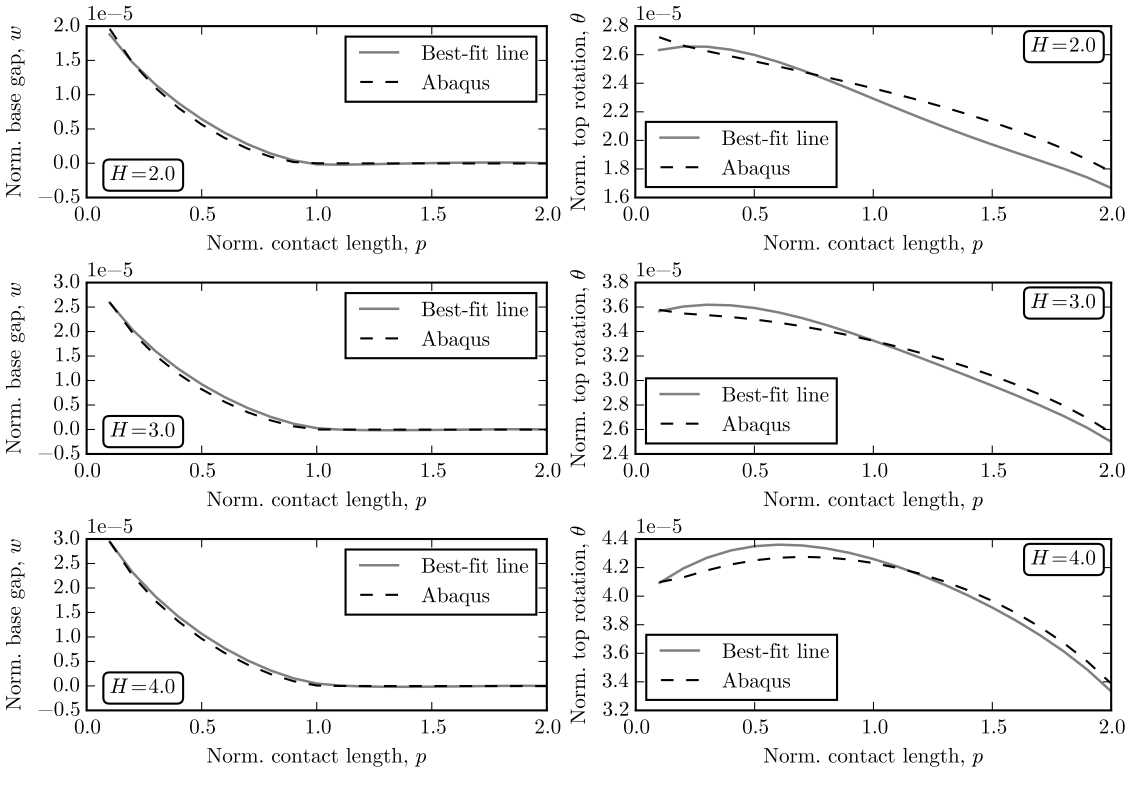

Figure 5: Rocking members with different heights loaded with a concentrated horizontal force on their top: Central gap and top rotation versus the contact length at the bottom, p, and for $s = -1000, E = 30000000, \nu = 0.2$

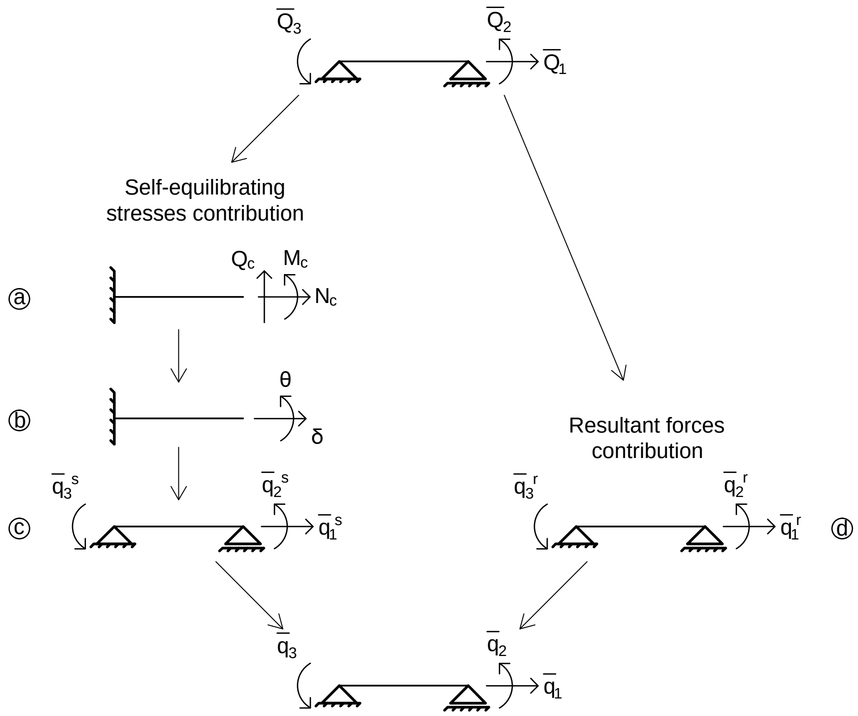

Figure 6: Schematic procedure used to calculate the combined displacements $\bar{\boldsymbol{q}}$ from the forces $\bar{\boldsymbol{Q}}$

Additionally, the problem that was formulated in section 2 referred to a semi-infinite strip of normalized semi-width $b = 1$, thickness $W = 1$ and stress distributions defined in the range $[-1, p-1]$. So, this problem has to be generalized to cover random width B, thickness W and load direction cases.

The conversion of the simply supported beam forces, $\bar{\boldsymbol{Q}} = [\bar{Q}_1, \bar{Q}_2, \bar{Q}_3]^T$, to the normalized problem cantilever ones, $\bar{\boldsymbol{Q}}_{\boldsymbol{c}} = [N_c, M_c, Q_c]^T$ (Fig. 6a), to the corresponding stress load parameters, $\boldsymbol{R_c} = [c, s, t']^T$, and finally to normalized problem stress load parameters, $\boldsymbol{R} = [p, s, t]^T$, is described by the following equations:

$$\bar{\boldsymbol{Q}}_{\boldsymbol{c}} = \boldsymbol{S_1}\bar{\boldsymbol{Q}} \tag{7}$$

$$\boldsymbol{R_c} = \begin{Bmatrix} 3\left(b + \dfrac{|M_c|}{N_c}\right) \\ \dfrac{2}{3}\dfrac{N_c}{b + \frac{|M_c|}{N_c}} \\ \dfrac{1}{2}\dfrac{Q_c}{b + \frac{|M_c|}{N_c}} \end{Bmatrix} \text{ with } N_c < 0 \tag{8}$$

$$\boldsymbol{R} = \boldsymbol{S_2}\boldsymbol{R_c} \tag{9}$$

where

$$\boldsymbol{S_1} = \frac{1}{W}\begin{bmatrix} 1 & 0 & 0 \\ 0 & 1 & 0 \\ 0 & -\dfrac{1}{L} & -\dfrac{1}{L} \end{bmatrix} \quad \boldsymbol{S_2} = \begin{bmatrix} \dfrac{1}{b} & 0 & 0 \\ 0 & 1 & 0 \\ 0 & 0 & \rho \end{bmatrix} \text{ and } \rho = \text{sign}(M_c) \tag{10}$$

Similarly, after the calculation of the displacements $\boldsymbol{U} = [\delta, \theta]^T$ of the normalized problem (Fig. 6b), the conversion to the ones of the general simply supported beam problem, $\bar{\boldsymbol{q}} =$

$[\bar{q}_1, \bar{q}_2, \bar{q}_3]^T$ (Fig. 6c), is described by the equation:

$$\boldsymbol{\bar{q}} = \boldsymbol{S_3 U} \tag{11}$$

where

$$\boldsymbol{S_3} = \begin{bmatrix} b & 0 \\ 0 & \rho \\ 0 & 0 \end{bmatrix} \tag{12}$$

The self-equilibrating part of the rocking element is active only if a portion of the section supported on the ground is active, that is, only if

$$c < B \Rightarrow \left| \frac{M_c}{N_c} \right| > \frac{b}{3} \tag{13}$$

which means that the resultant normal force must be located outside the kern of the section.

Also, given the flexibility matrix of the normalized semi-infinite strip problem $\boldsymbol{F_t} = \dfrac{\partial \boldsymbol{U}}{\partial \boldsymbol{R}}$, the flexibility matrix in the simply supported beam coordinate system $\dfrac{\partial \boldsymbol{\bar{q}}}{\partial \boldsymbol{\bar{Q}}}$ is evaluated as follows:

$$\frac{\partial \boldsymbol{\bar{q}}}{\partial \boldsymbol{\bar{Q}}} = \frac{\partial \boldsymbol{\bar{q}}}{\partial \boldsymbol{U}} \frac{\partial \boldsymbol{U}}{\partial \boldsymbol{R}} \frac{\partial \boldsymbol{R}}{\partial \boldsymbol{R_c}} \frac{\partial \boldsymbol{R_c}}{\partial \boldsymbol{\bar{Q}_c}} \frac{\partial \boldsymbol{\bar{Q}_c}}{\partial \boldsymbol{\bar{Q}}} = \boldsymbol{S_3}\ \boldsymbol{F_t}\ \boldsymbol{S_2}\ \boldsymbol{S_4}\ \boldsymbol{S_1} \tag{14}$$

with

$$\boldsymbol{S_4} = \frac{\partial \boldsymbol{R_c}}{\partial \boldsymbol{\bar{Q}_c}} = \begin{bmatrix} -3\dfrac{|M_c|}{N_c^2} & 3\dfrac{\rho}{N_c} & 0 \\ \dfrac{2}{3}\dfrac{b + 2\frac{|M_c|}{N_c}}{\left(b + \frac{|M_c|}{N_c}\right)^2} & -\dfrac{2}{3}\dfrac{\rho}{\left(b + \frac{|M_c|}{N_c}\right)^2} & 0 \\ \dfrac{1}{2}\dfrac{|M_c|Q_c}{(N_c b + |M_c|)^2} & -\dfrac{1}{2}\dfrac{\rho N_c Q_c}{(N_c b + |M_c|)^2} & \dfrac{1}{2}\dfrac{1}{b + \frac{|M_c|}{N_c}} \end{bmatrix} = \begin{bmatrix} -3\dfrac{|M_c|}{N_c^2} & 3\dfrac{\rho}{N_c} & 0 \\ \dfrac{4}{c} - \dfrac{6b}{c^2} & -6\dfrac{\rho}{c^2} & 0 \\ \dfrac{9}{2}\dfrac{|M_c|Q_c}{N_c^2 c^2} & -\dfrac{9}{2}\dfrac{\rho Q_c}{N_c c^2} & \dfrac{3}{2c} \end{bmatrix} \tag{15}$$

The contribution of the resultant forces can be calculated as usual. The flexibility matrix of the elastic simply supported beam, taking into account shear deformation effects, is (e.g. [31]):

$$\boldsymbol{F_r} = \begin{bmatrix} \dfrac{L}{EA} & 0 & 0 \\ 0 & \dfrac{L}{3EI} + \dfrac{\alpha}{GAL} & -\dfrac{L}{6EI} + \dfrac{\alpha}{GAL} \\ 0 & -\dfrac{L}{6EI} + \dfrac{\alpha}{GAL} & \dfrac{L}{3EI} + \dfrac{\alpha}{GAL} \end{bmatrix} \tag{16}$$

where α is the shear shape factor with $\alpha \approx 1.2$ for rectangular cross sections (shear deformations contribution can be neglected by setting $\alpha = 0.0$). So, the displacements at the nodes originating from the resultant forces (Fig. 6d) are given by

$$\boldsymbol{\bar{q}_r} = \boldsymbol{F_r \bar{Q}} \tag{17}$$

The general algorithm for the macro-element which combines these two contributions, based on the algorithm in [30], is presented in table 2, where index r refers to the resultant force problem and s refers to the self-equilibrating stress problem (extended semi-infinite strip algorithm).

Table 2: Rocking macro-element algorithm

1. Elimination of rigid body modes	$\bar{\boldsymbol{q}}_i = \boldsymbol{T}_i \boldsymbol{q}_i$ $\Delta\bar{\boldsymbol{q}}_i = \boldsymbol{T}_i \Delta\boldsymbol{q}_i$
2. Nodal force increments	$\Delta\bar{\boldsymbol{Q}}_i = \boldsymbol{F}_{i-1}^{-1}\Delta\bar{\boldsymbol{q}}_i$
3. Nodal forces	$\bar{\boldsymbol{Q}}_i = \bar{\boldsymbol{Q}}_{i-1} + \Delta\bar{\boldsymbol{Q}}_i$
4. Flexibility matrix and Nodal displacements for the resultant force problem	$\bar{\boldsymbol{q}}_{\boldsymbol{r}}^* = \boldsymbol{F}_{\boldsymbol{r}}\bar{\boldsymbol{Q}}_i$
5. Check whether there is rocking or not. If not, ignore steps (6)-(10) and set $\bar{\boldsymbol{q}}_{\boldsymbol{s}}^*$ and $\boldsymbol{F}_{\boldsymbol{s}}$ to the zero matrices	$\left\lvert\frac{\bar{Q}_2}{\bar{Q}_1}\right\rvert > \frac{b}{3} \rightarrow$ Rocking
6. Force parameters for the self-equilibrating stresses problem	$\bar{\boldsymbol{Q}}_{\boldsymbol{c}} = \boldsymbol{S}_{\boldsymbol{1}}\bar{\boldsymbol{Q}}_i$ $\boldsymbol{R}_{\boldsymbol{c}} = \boldsymbol{R}_{\boldsymbol{c}}(\bar{\boldsymbol{Q}}_{\boldsymbol{c}})$ $\boldsymbol{R} = \boldsymbol{S}_{\boldsymbol{2}}\boldsymbol{R}_{\boldsymbol{c}}$
7. Displacements of the normalized problem	$\boldsymbol{U} = \boldsymbol{G}\ \boldsymbol{L}$
8. Displacements in the simply-supported beam natural system	$\bar{\boldsymbol{q}}_{\boldsymbol{s}}^* = \boldsymbol{S}_{\boldsymbol{3}}\ \boldsymbol{U}$
9. Flexibility matrix of the normalized problem	$\boldsymbol{F}_{\boldsymbol{t}} = \frac{\partial \boldsymbol{U}}{\partial \boldsymbol{R}}$
10. Flexibility matrix in the simply-supported beam natural system	$\boldsymbol{F}_{\boldsymbol{s}} = \boldsymbol{S}_{\boldsymbol{3}}\ \boldsymbol{F}_{\boldsymbol{t}}\ \boldsymbol{S}_{\boldsymbol{2}}\ \boldsymbol{S}_{\boldsymbol{4}}\ \boldsymbol{S}_{\boldsymbol{1}}$
11. Combined displacements	$\bar{\boldsymbol{q}}_i^* = \bar{\boldsymbol{q}}_{\boldsymbol{r}}^* + \bar{\boldsymbol{q}}_{\boldsymbol{s}}^*$
12. Displacement residuals	$\boldsymbol{r}_i = \bar{\boldsymbol{q}}_i - \bar{\boldsymbol{q}}_i^*$
13. Combined flexibility matrix	$\boldsymbol{F}_i = \boldsymbol{F}_{\boldsymbol{r}} + \boldsymbol{F}_{\boldsymbol{s}}$
14. Extra nodal forces	$\bar{\boldsymbol{Q}}_i^* = \boldsymbol{F}_i^{-1}\boldsymbol{r}_i$
15. Updated nodal forces	$\bar{\boldsymbol{Q}}_i = \bar{\boldsymbol{Q}}_i + \bar{\boldsymbol{Q}}_i^*$
16. *(Optional)* Check convergence	$\frac{\lvert\bar{\boldsymbol{Q}}_i^*\rvert}{\lvert\bar{\boldsymbol{Q}}_i^{old}\rvert} >$ error $\Rightarrow$ return to step 4
17. Inclusion of rigid body modes	$\boldsymbol{Q}_i = \boldsymbol{T}^*\bar{\boldsymbol{Q}}_i$ $\boldsymbol{K}_i = \boldsymbol{T}_{1i} + \boldsymbol{T}_{\boldsymbol{i}}^*\boldsymbol{F}_i^{-1}\boldsymbol{T}_{\boldsymbol{i}}^{*\boldsymbol{T}}$

4 EXAMPLES

As a first example, the response of a simple cantilever model is calculated using the proposed macro-element. The results are compared with the results of the corresponding Abaqus model, consisting of 2D plane stress elements with contact properties at the base which allow only compressive stresses to develop.

In Fig. 7, a cantilever with height $H = 2$ m, width $B = 1$ m and thickness $W = 0.2$ m is examined, which is loaded with a vertical force $N = -400$ kN. In Fig. 7a, the pushover curves of such cantilevers with various E values and $\nu = 0.2$ are shown together with the theoretical rigid block case. It can be seen that, due to the non-linearity of the response, the maximum strength achieved decreases with decreasing E values.

In Fig. 7b, the response of the body with $E = 30$ GPa case is examined more thoroughly: apart from a magnification of the pushover curve in the initial region, the top rotation and the vertical displacement at the center of the body with and without shear deformation effects are presented. Comparison of the results with the ones of the corresponding Abaqus model shows

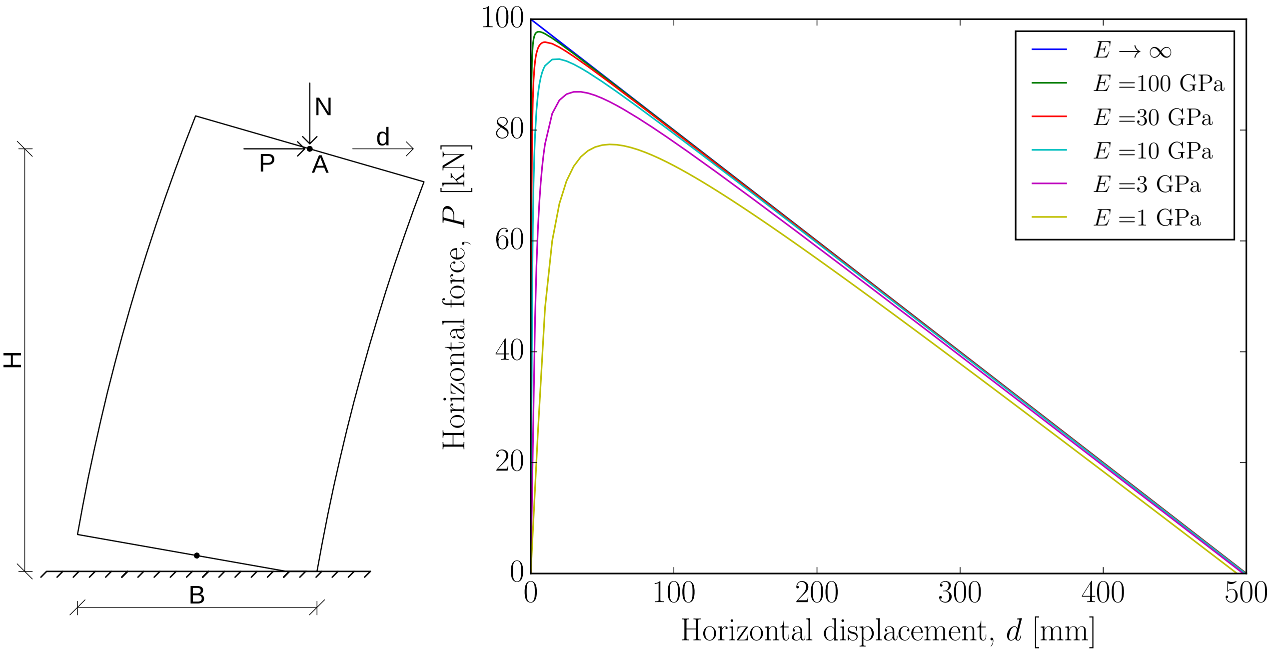

(a)

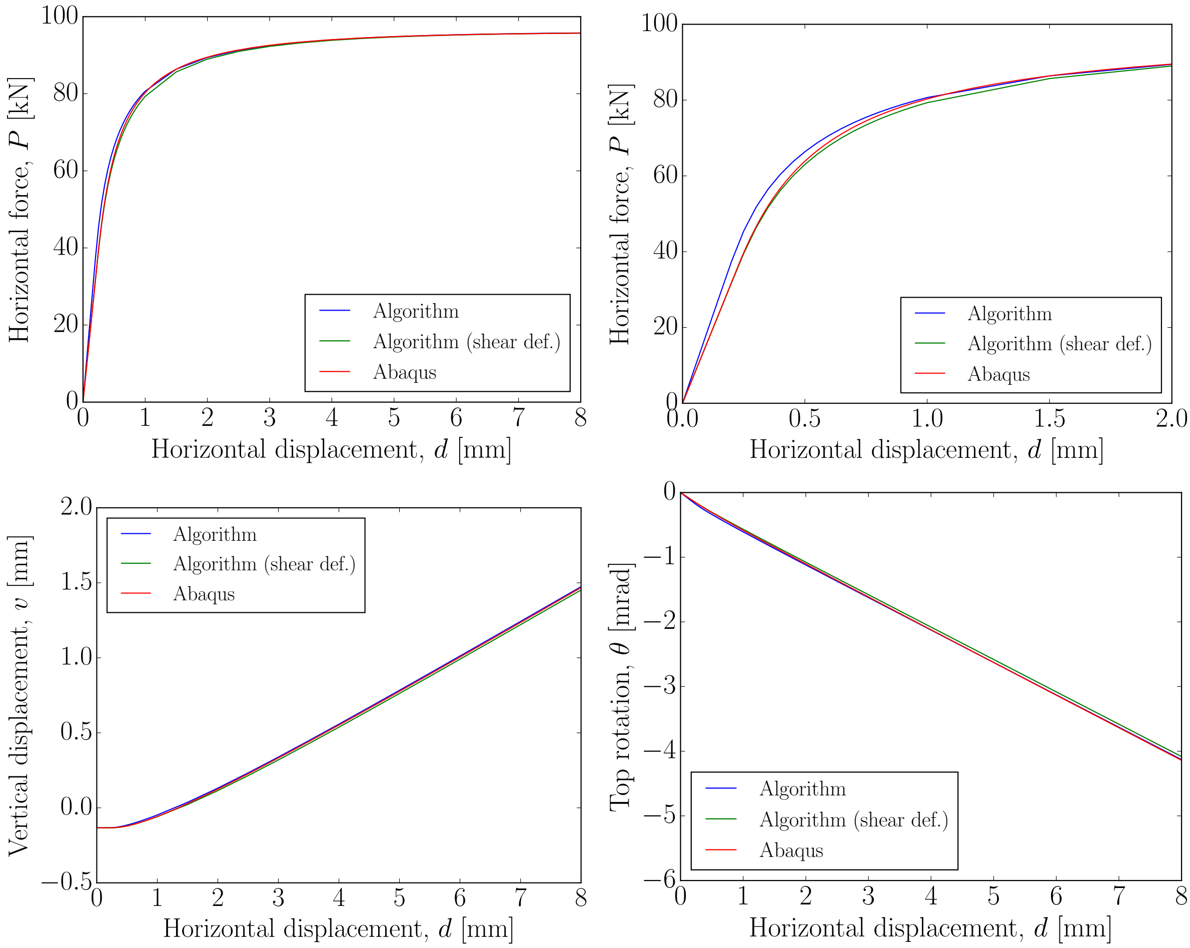

(b)

Figure 7: Example 1, $H = 2$ m panel loaded with vertical force $N = -400$ kN and horizontal force P at its top: (a) Pushover curves for different E values; (b) Pushover curves, top rotation and vertical displacement for the $E = 30$ GPa case, which is also compared with the corresponding Abaqus model

that, generally, the proposed macro-element can predict the response very accurately, especially if shear deformations are considered.

As a second example, the rocking body is examined with an elastic tendon with Young's modulus E_t and section area A_t installed along its center-line, imposing a prestress force with initial value $P_{t0} = 400$ kN. In this way, the vertical displacements are restrained after the onset of rocking, while the axial force originating from the tendon increases as its elongation increases.

The results are shown in Fig. 8 for typical values of tendon coefficients E_tA_t. It can be seen that the prestressing tendons force the pushover curve to be ascending instead of descending, offering stability to the system.

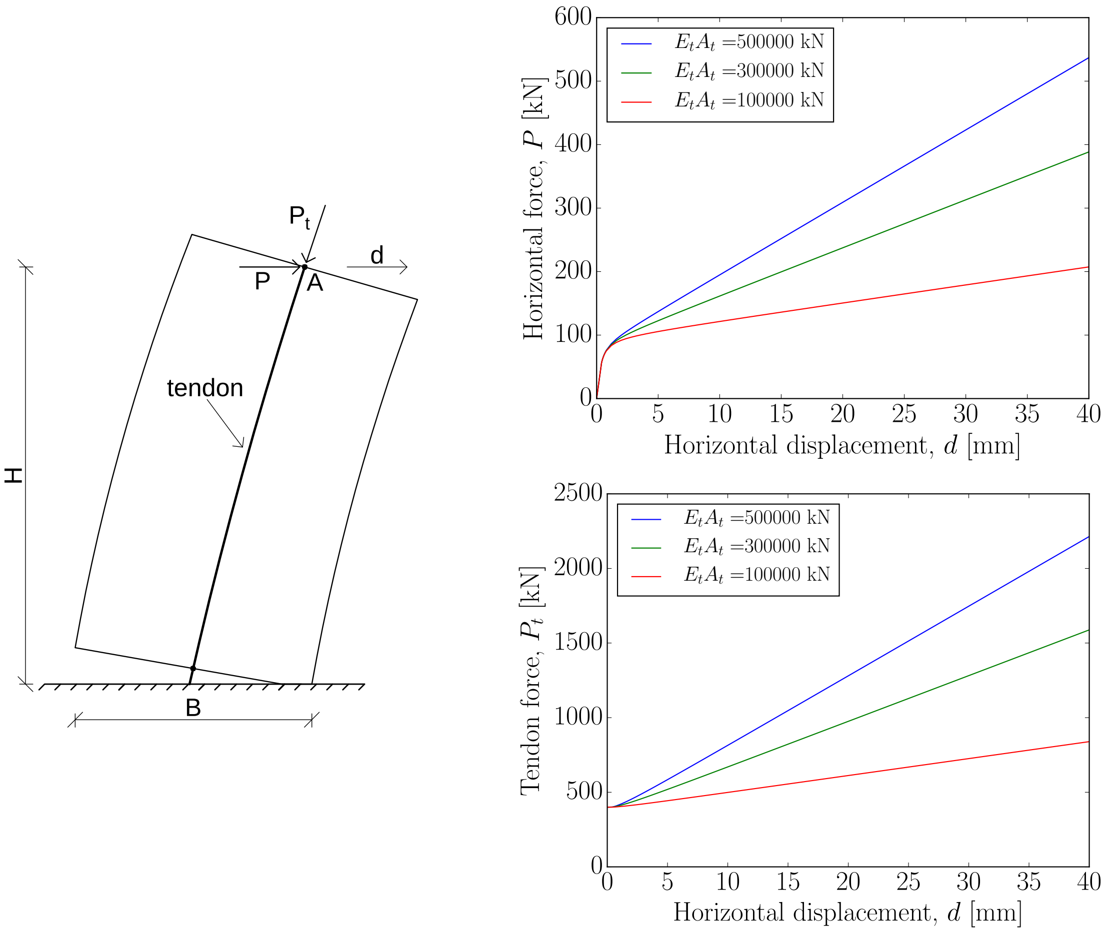

Figure 8: Example 2, $H = 2$ m panel with a horizontal force P at its top, constrained with a tendon with Young's modulus E_t, section area A_t and prestress force $P_{t0} = 400kN$: Pushover curve and tendon force

5 CONCLUSIONS

In this paper, a new macro-element algorithm is proposed, which can be used for the calculation of the rocking response of flexible bodies, also accounting for the deformability of their base. This is crucial in case of restrained rocking, when considerable axial forces develop. The formulation of the element is based upon the solution of the normalized semi-infinite strip problem, in order to account for the partial loading imposed on the rocking interface.

Two example problems are presented, showing typical cases where the proposed element can be used. Comparison of the results with ones obtained using equivalent Abaqus models shows very good agreement between the two methods, while the proposed algorithm requires extremely low runtimes compared to conventional finite element codes.

ACKNOWLEDGEMENTS

The first author would like to thank the Greek State Scholarships Foundation for its financial support through the "IKY Fellowships of Excellence for Postgraduate studies in Greece - Siemens program".

REFERENCES

[1] R. Skinner, R. Tyler, A. Heine, and W. Robinson, "Hysteretic dampers for the protection of structures from earthquakes," *Bulletin of the New Zealand National Society for Earthquake Engineering*, vol. 13, no. 1, pp. 22–36, 1980.

[2] N. M. Priestley, "Overview of PRESSS research program," *PCI journal*, vol. 36, no. 4, 1991.

[3] S. Sritharan, S. Aaleti, and D. J. Thomas, "Seismic analysis and design of precast concrete jointed wall systems," *ISU-ERI-Ames Report ERI-07404, Submitted to the Precast/Prestressed Concrete Institute*, 2007.

[4] W. Y. Kam, S. Pampanin, A. Palermo, and A. J. Carr, "Self-centering structural systems with combination of hysteretic and viscous energy dissipations," *Earthquake Engineering & Structural Dynamics*, vol. 39, no. 10, pp. 1083–1108, 2010.

[5] ACI Innovation Task Group 1, "Special Hybrid Moment Frames Composed of Discretely Jointed Precast and Post-Tensioned Concrete Members (ACI T1.2-03) and Commentary (ACI T1.2R-03)," American Concrete Institute (ACI), 2003.

[6] "Seismic design of precast concrete building structures," *fib Bulletin no. 27*, International Federation for Structural Concrete (fib), 2003.

[7] "Special provisions for the seismic design of ductile jointed precast concrete structural systems," *NZS3101: 2006, Concrete Standards, Appendix B*, New Zealand Standards, 2006.

[8] "Eurocode 8: Design of structures for earthquake resistance Part 1: General rules, seismic actions and rules for buildings," *European Standard EN 1998-1:2004*, European Committee for Standardization, 2004.

[9] G. W. Housner, "The behavior of inverted pendulum structures during earthquakes," *Bulletin of the seismological society of America*, vol. 53, no. 2, pp. 403–417, 1963.

[10] C.-S. Yim, A. K. Chopra, and J. Penzien, "Rocking response of rigid blocks to earthquakes," *Earthquake Engineering and Structural Dynamics*, vol. 8, no. 6, pp. 565–587, 1980.

[11] J. Zhang and N. Makris, "Rocking response of free-standing blocks under cycloidal pulses," *Journal of Engineering Mechanics*, vol. 127, no. 5, pp. 473–483, 2001.

[12] E. G. Dimitrakopoulos and M. J. DeJong, "Revisiting the rocking block: closed-form solutions and similarity laws," in *Proceedings of the Royal Society of London A: Mathematical, Physical and Engineering Sciences*, vol. 468, pp. 2294–2318, The Royal Society, 2012.

[13] S. Acikgoz and M. J. DeJong, "The interaction of elasticity and rocking in flexible structures allowed to uplift," *Earthquake Engineering & Structural Dynamics*, vol. 41, no. 15, pp. 2177–2194, 2012.

[14] C. B. Barthes, *Design of Earthquake Resistant Bridges Using Rocking Columns*. PhD thesis, University of California, Berkeley, 2012.

[15] M. F. Vassiliou, K. R. Mackie, and B. Stojadinović, "Dynamic response analysis of solitary flexible rocking bodies: modeling and behavior under pulse-like ground excitation," *Earthquake Engineering & Structural Dynamics*, vol. 43, no. 10, pp. 1463–1481, 2014.

[16] M. F. Vassiliou, R. Truniger, and B. Stojadinović, "An analytical model of a deformable cantilever structure rocking on a rigid surface: development and verification," *Earthquake Engineering & Structural Dynamics*, 2015.

[17] I. N. Psycharis and P. C. Jennings, "Rocking of slender rigid bodies allowed to uplift," *Earthquake Engineering & Structural Dynamics*, vol. 11, no. 1, pp. 57–76, 1983.

[18] I. N. Psycharis, "Dynamics of flexible systems with partial lift-off," *Earthquake Engineering & Structural Dynamics*, vol. 11, no. 4, pp. 501–521, 1983.

[19] A. K. Chopra and S. C.-S. Yim, "Simplified earthquake analysis of structures with foundation uplift," *Journal of Structural Engineering*, vol. 111, no. 4, pp. 906–930, 1985.

[20] I. N. Psycharis, "Effect of base uplift on dynamic response of sdof structures," *Journal of Structural Engineering*, vol. 117, no. 3, pp. 733–754, 1991.

[21] A. Palmeri and N. Makris, "Response analysis of rigid structures rocking on viscoelastic foundation," *Earthquake Engineering & Structural Dynamics*, vol. 37, no. 7, pp. 1039–1063, 2008.

[22] A. Palmeri and N. Makris, "Linearization and first-order expansion of the rocking motion of rigid blocks stepping on viscoelastic foundation," *Earthquake Engineering & Structural Dynamics*, vol. 37, no. 7, pp. 1065–1080, 2008.

[23] H. Roh and A. M. Reinhorn, "Analytical modeling of rocking elements," *Engineering Structures*, vol. 31, no. 5, pp. 1179–1189, 2009.

[24] H. Roh and A. M. Reinhorn, "Nonlinear static analysis of structures with rocking columns," *Journal of structural engineering*, vol. 136, no. 5, pp. 532–542, 2009.

[25] H. Roh and A. M. Reinhorn, "Modeling and seismic response of structures with concrete rocking columns and viscous dampers," *Engineering Structures*, vol. 32, no. 8, pp. 2096–2107, 2010.

[26] A. Belleri, M. Torquati, and P. Riva, "Finite element modeling of rocking walls," in *4th ECCOMAS Them. Conf. on COMPDYN*, 2013.

[27] A. Penna, S. Lagomarsino, and A. Galasco, "A nonlinear macroelement model for the seismic analysis of masonry buildings," *Earthquake Engineering & Structural Dynamics*, vol. 43, no. 2, pp. 159–179, 2014.

[28] E. Avgenakis, "Modeling of rocking flexible bodies considering the deformability of their base," Master's thesis, National Technical University of Athens, 2015.

[29] F. Gaydon and W. Shepherd, "Generalized plane stress in a semi-infinite strip under arbitrary end-load," in *Proceedings of the Royal Society of London A: Mathematical, Physical and Engineering Sciences*, vol. 281, pp. 184–206, The Royal Society, 1964.

[30] A. Neuenhofer and F. C. Filippou, "Geometrically nonlinear flexibility-based frame finite element," *Journal of Structural Engineering*, vol. 124, no. 6, pp. 704–711, 1998.

[31] J. S. Przemieniecki, *Theory of matrix structural analysis*. Courier Corporation, 1985.